

Light-Meson Spectroscopy at Lepto- and Hadroproduction Experiments

B. Grube*

*Institute for Hadronic Structure and Fundamental Symmetries,
Technische Universität München, Garching, Germany*

**E-mail: bgrube@tum.de*

The excitation spectrum of light mesons, which are composed of up, down, and strange quarks, is studied since decades. However, it still holds a number of puzzles and surprises that provide new insights into the nature of the strong interaction. Recent high-quality data samples from several experiments allow us to not only study the properties of established mesons with unprecedented precision but to also search for new states. These searches aim in particular at resolving the question of the existence of so-called exotic states, such as four-quark states or states with excited gluon fields. Since light mesons have often large widths and are overlapping, the mapping of their spectrum is challenging and requires large quantities of data on different production and decay modes. The data are analyzed using a framework of interfering quantum mechanical amplitudes known as partial-wave analysis (PWA). Most excited meson states decay into multi-particle final states, for which the PWA requires extensive modeling of the dynamics of the final-state hadrons. I will give an overview on ongoing experimental studies of light mesons and discuss possible interpretations. I will also touch on novel analysis techniques and the prospects for future progress.

1. Introduction

The precision measurement of the spectrum of light mesons is the aim of several experiments. The focus of these experiments lies in particular on confirming and finding new highly excited states, on completing $SU(3)_{\text{flavor}}$ multiplets, and on searching for exotic mesons, i.e., states that cannot be composed of (just) $q\bar{q}'$. These data provide important input for theory and phenomenology and eventually help to better understand the nature of confinement. The current analyses in the field are driven not only by the high-quality data from experiments, but also by the development and application of advanced analysis techniques and of more rigorous theoretical models for partial-wave analyses (PWA).

2. Spin-Exotic Light Mesons

Spin-exotic mesons have J^{PC} quantum numbers^a of 0^{--} , $(2n)^{+-}$, or $(2n+1)^{-+}$ with $n \in \mathbb{N}$ that are forbidden for $|q\bar{q}\rangle$ states in the non-relativistic limit. In the light-meson sector, so far three spin-exotic candidate states—all with $J^{PC} = 1^{-+}$ —have been claimed by experiments:¹ $\pi_1(1400)$, $\pi_1(1600)$, and $\pi_1(2100)$. The latter one has been observed only by the BNL E852 experiment and needs confirmation.

2.1. 3π Final State

Some of the experimental claims are controversial, in particular the observation of the $\pi_1(1600)$ in the $\rho(770)\pi$ decay. The BNL E852 experiment claimed a $\pi_1(1600)$ signal in a PWA of 2.5×10^5 3π events diffractively produced by an 18 GeV/c π^- beam on a proton target. The PWA was performed in the range from 0.1 to 1.0 (GeV/c)² of the reduced four-momentum transfer squared t' using a PWA model containing 21 waves.^{2,3} However, in a later analysis of a more than ten times larger data sample of 2.6×10^6 3π events no evidence for the $\pi_1(1600)$ was found.⁴ However, the non-observation claim was based on data in the narrower range $0.1 < t' < 0.5$ (GeV/c)².

Recently, the COMPASS experiment at CERN⁵ published results of a PWA of a large data sample of 4.6×10^7 3π events diffractively produced by a 190 GeV/c π^- beam on a proton target in the range $0.1 < t' < 1.0$ (GeV/c)².^{6,7} The employed PWA model contains 88 partial waves and is an extension of the 36-wave set used in Ref. [4]. The PWA was performed in 11 narrow t' intervals. Figures 1a and 1b show the measured intensity distributions (black points) of the spin-exotic 1^{-+} $\rho(770)\pi$ P -wave for the lowest and the highest t' bin. Surprisingly, the shape of the intensity distribution changes drastically with increasing t' . At low t' , COMPASS observes a broad distribution, whereas at high t' , a peak emerges at 1.6 GeV/c². This suggests that the partial-wave amplitude has large t' -dependent contributions from non-resonant processes. The continuous curves in Fig. 1 represent a resonance-model fit, where the partial-wave amplitude is modeled as the coherent sum (red curves) of a Breit-Wigner amplitude for the $\pi_1(1600)$ (blue curves) and a non-resonant amplitude (green curves). The modulation of the intensity distribution with t' is well reproduced by the model. At low t' , the intensity is described mostly by the non-resonant

^aHere, J is the meson spin and P and C are the eigenvalues of parity and charge conjugation, respectively.

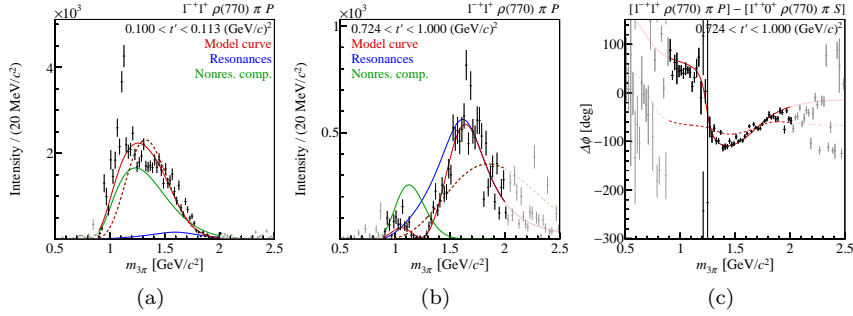


Figure 1. (a) and (b): Intensity distributions of the $1^{-+} \rho(770)\pi$ P -wave in the COMPASS $\pi^{-}\pi^{-}\pi^{+}$ proton-target data in the lowest and highest t' bin, respectively. (c) Phase of this wave relative to the $1^{++} \rho(770)\pi$ S -wave in the highest t' bin. From Ref. [7].

component (green curve), whereas the peak at high t' is described nearly completely by the Breit-Wigner component of the model (blue curve). The measured $\pi_1(1600)$ Breit-Wigner parameters are $m_0 = 1600^{+110}_{-60} \text{ MeV}/c^2$ and $\Gamma_0 = 580^{+100}_{-230} \text{ MeV}/c^2$. That a resonance is indeed required to describe the data, is demonstrated by a fit, where the $\pi_1(1600)$ component is removed from the resonance model (red dashed curves in Fig. 1) leaving only the non-resonant component in this wave. Using the so-called freed-isobar PWA approach, it was also verified that the observed $\pi_1(1600)$ signal is not an artifact caused by inadequate isobar parameterizations (see Ref. [8] for details).

Performing the PWA and the resonance-model fit in narrow t' bins hence resolves the long-standing puzzle of the seemingly contradictory results obtained by the BNL E852 experiment. Using an even larger wave set than the BNL analyses, the COMPASS results confirm that the prominent peak reported in the first BNL analysis in Refs. [2, 3] is an artifact caused by a too small wave set. The non-observation of the $\pi_1(1600)$ reported in the second BNL analysis in Ref. [4] is explained by the exceptionally steep t' dependence of the non-resonant component. In the range $t' \lesssim 0.5 \text{ (GeV/c)}^2$, the non-resonant component dominates and the COMPASS data show only a small $\pi_1(1600)$ signal, which becomes prominent only for $t' \gtrsim 0.5 \text{ (GeV/c)}^2$. Hence the non-observation of the $\pi_1(1600)$ in the second BNL analysis was mainly a result of the analyzed t' range.

A remaining puzzle is that although the $\pi_1(1600)$ decays into $\rho(770)\pi$, it does not seem to be observed in photoproduction.^{9–11} In the future, much more precise photoproduction data from the GlueX and MesonX experiments at JLab will help to clarify the situation.

2.2. $\eta\pi$ and $\eta'\pi$ Final States

Other interesting final states to search for spin-exotic mesons are $\eta\pi$ and $\eta'\pi$. In contrast to the analysis of three-body final states, where PWA models usually employ the isobar model thereby introducing a large model dependence, the PWA of two-body final states does not require such strong model assumptions. In the $\eta^{(\prime)}\pi$ system, partial waves that correspond to non-zero, odd orbital-angular momentum between the $\eta^{(\prime)}$ and the π correspond to spin-exotic quantum numbers. The lowest such wave is the P -wave with $J^{PC} = 1^{-+}$. Previous experiments have observed the $\pi_1(1400)$ in the $\eta\pi$ P -wave and the $\pi_1(1600)$ in the $\eta'\pi$ P -wave.¹

Recently, members of the Joint Physics Analysis Center (JPAC) have performed a coupled-channel fit of the $\eta\pi$ and $\eta'\pi$ P - and D -wave amplitudes extracted from COMPASS data¹² using a unitary model based on S -matrix principles.¹³ They find two resonance poles, the $a_2(1320)$ and the $a_2(1700)$, in the D -wave amplitudes and a single pole in the P -wave amplitudes. The pole parameters of $m_0 = 1564 \pm 24$ (stat.) ± 86 (sys.) MeV/ c^2 and $\Gamma_0 = 492 \pm 54$ (stat.) ± 102 (sys.) MeV/ c^2 are consistent with the $\pi_1(1600)$.

This result is in so far remarkable as only a single pole is required to describe both the $\eta\pi$ and the $\eta'\pi$ P -wave amplitudes despite their rather different intensity distributions (see Fig. 2). As mentioned above, this is in contrast to most previous analyses, where the broad peak at 1.4 GeV/ c^2 in the $\eta\pi$ P -wave intensity was described by the $\pi_1(1400)$ whereas the narrower peak at 1.6 GeV/ c^2 in the $\eta'\pi$ P -wave intensity, which is nearly identical to the peak observed in the high t' region of the $\pi^-\pi^-\pi^+$ data, was described by the $\pi_1(1600)$. As the COMPASS data are similar to those of previous experiments, the JPAC analysis raises doubts about the existence of the $\pi_1(1400)$ as a separate resonance. This would resolve the longstanding puzzle of two spin-exotic states lying unexpectedly close to each other. If interpreted as hybrid states, this would also remove the discrepancy with lattice QCD and most model calculations, which predict the lightest hybrid state to have a mass

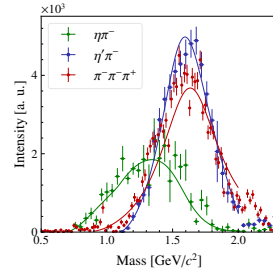


Figure 2. Comparison of COMPASS data: Intensity distributions of the $\eta\pi$ (green points) and $\eta'\pi$ (blue points) P -wave¹² for $0.1 < t' < 1.0$ (GeV/ c)² and of the $1^{-+} \rho(770)\pi$ P -wave in the $\pi^-\pi^-\pi^+$ data for $0.449 < t' < 0.724$ (GeV/ c)² (red points). The curves represent the fit results from Refs. [7, 13].

substantially higher than that of the $\pi_1(1400)$ (see e.g., Ref. [14]).

2.3. *GlueX Data*

The GlueX experiment at JLab¹⁵ uses a linearly polarized photon beam to study photoproduction of light mesons on a proton target. The main goal is a precision measurement of the light-meson spectrum in the mass range $\lesssim 3 \text{ GeV}/c^2$ and in particular the search for hybrid mesons. The maximum photon polarization is reached at a photon energy of about 9 GeV. In this energy range, various exchange processes contribute and states with a wide variety of $I^G J^{PC}$ quantum numbers^b are accessible. The photon polarization helps to disentangle these production processes. GlueX is hence complementary to high-energy pion-scattering experiments such as COMPASS, where only states with $I^G = 1^-$ are produced directly.

GlueX has finished its first phase of data taking and has acquired world leading data samples for many final states. First analyses showcase the potential of these data.^{16,17} As an example, Fig. 3 shows kinematic distributions for the reaction $\gamma p \rightarrow \eta \pi^- \Delta^{++}$ with $\eta \rightarrow \gamma \gamma$. The $\eta \pi$ invariant mass distribution in Fig. 3a exhibits clear peaks of $a_0(980)$ and $a_2(1320)$. This is also consistent with the angular distribution shown in Fig. 3b. The band in the $a_0(980)$ region is approximately independent of the angle indicating a spin-0 resonance, whereas the $a_2(1320)$ region shows the expected 2-bump behaviour. In total, about 10^6 $\eta \pi$ events are expected in this channel, which is about 10 times the size of the COMPASS data sample. The second data-taking campaign of GlueX that started fall 2019 is expected to enlarge the data samples by another factor of 4 to 5.

3. Kaon Spectroscopy

In order to better understand the light-meson spectrum it is important to complete the $\text{SU}(3)_{\text{flavor}}$ nonets. However, the kaon spectrum is not well known. Currently, the PDG lists only 25 kaon states, 12 of which need confirmation.¹

The COMPASS experiment has measured kaon diffraction on a proton target using the 2.4% K^- component in the 190 GeV/c hadron beam. In particular, COMPASS has acquired the so far largest data sample of 720 000 events of the reaction $K^- p \rightarrow K^- \pi^- \pi^+ p$.¹⁸ The invariant mass distribution of the $K^- \pi^- \pi^+$ system shown in Fig. 4a exhibits possible

^bHere, I is the isospin and G the G -parity.

6

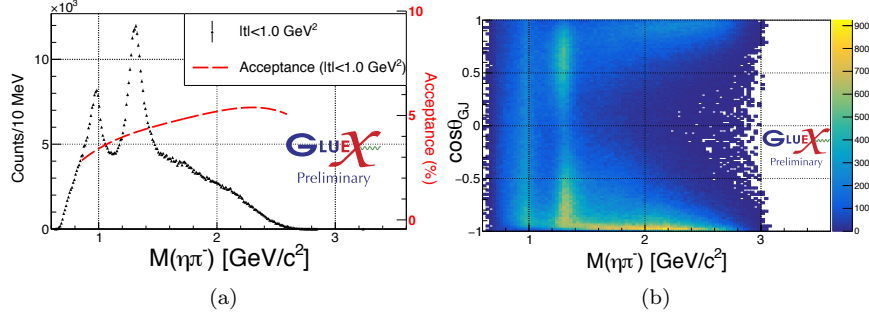


Figure 3. (a) Invariant mass distribution of the $\eta\pi^-$ system produced in the reaction $\gamma p \rightarrow \eta\pi^- \Delta^{++}$ as measured by the GlueX experiment.¹⁷ (b) Distribution of the cosine of the polar angle of the η with respect to the beam photon in the $\eta\pi$ rest frame vs. the $\eta\pi$ mass.

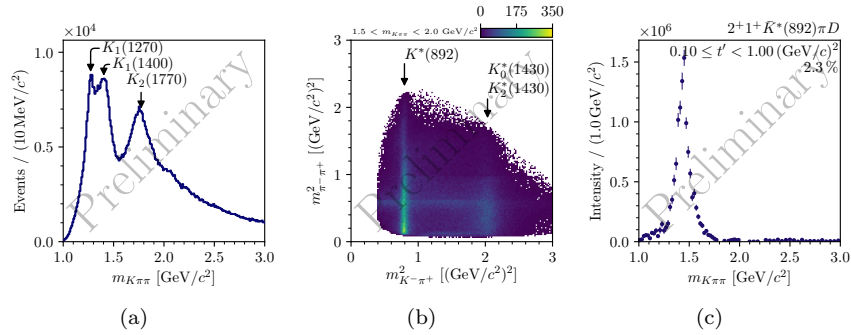


Figure 4. (a) $K^-\pi^-\pi^+$ invariant mass distribution with potential resonance signals indicated. (b) Dalitz plot around $m_{K^-\pi^-\pi^+} = 1.75 \text{ GeV}/c^2$. (c) Intensity distribution of the $J^P = 2^+$ wave decaying into $K^*(892)$ and π^- in a D -wave.

signals of known kaon resonances. The Dalitz plot in Fig. 4b around $m_{K^-\pi^-\pi^+} = 1.75 \text{ GeV}/c^2$ shows rich structures with signals of $\rho(770)$ and $f_0(980)$ in the $\pi^-\pi^+$ subsystem and of $K^*(892)$, $K_0^*(1430)$, and/or $K_2^*(1430)$ in the $K^-\pi^+$ subsystem.

A first PWA of these data was performed using a wave set determined by employing regularization techniques.¹⁹ To exemplify the potential of the COMPASS data, Fig. 4c shows the intensity of the $J^P = 2^+$ wave decaying into $K^*(892)$ and π^- in a D -wave, which exhibits a nearly background-free signal of the $K_2^*(1430)$. More details can be found in Ref. [18].

4. Summary

Light-meson spectroscopy has entered the era of high-precision data. These data reveal new details of the light-meson spectrum and help to settle some of the controversies of the past. The currently running GlueX and VES experiments and the soon to start MesonX experiment will provide even more precise data on various final states. In the more distant future, the PANDA experiment will also contribute to this field.

However, the PWA results from these large data samples become increasingly dominated by systematic uncertainties. A large contribution to these uncertainties comes from the model assumptions employed in the PWA of multi-body final states. Reducing these systematic uncertainties will require improved PWA models that respect fundamental physical principles such as analyticity and unitarity (see e.g., Ref. [20]). For scattering experiments, in addition the production processes needs to be better understood in order to improve the treatment of non-resonant processes, which are another source of large systematic uncertainties.

Bibliography

1. M. Tanabashi *et al.*, *Phys. Rev. D* **98**, 030001 (2018) and 2019 update.
2. G. S. Adams *et al.*, *Phys. Rev. Lett.* **81**, 5760 (1998).
3. S. U. Chung *et al.*, *Phys. Rev. D* **65**, 072001 (2002).
4. A. R. Dzierba *et al.*, *Phys. Rev. D* **73**, 072001 (2006).
5. P. Abbon *et al.*, *Nucl. Instr. Meth. A* **779**, 69 (2015).
6. C. Adolph *et al.*, *Phys. Rev. D* **95**, 032004 (2017).
7. M. Aghasyan *et al.*, *Phys. Rev. D* **98**, 092003 (2018).
8. F. Krinner, *in these proceedings*.
9. M. Nozar *et al.*, *Phys. Rev. Lett.* **102**, 102002 (2009).
10. P. Eugenio and C. Bookwalter, *AIP Conf. Proc.* **1560**, 421 (2013).
11. S. Grabmüller, PhD thesis, Technische Universität München, 2012. CERN-THESIS-2012-170.
12. C. Adolph *et al.*, *Phys. Lett. B* **740**, 303 (2015).
13. A. Rodas *et al.*, *Phys. Rev. Lett.* **122**, 042002 (2019).
14. C. A. Meyer and E. S. Swanson, *Prog. Part. Nucl. Phys.* **82**, 21 (2015).
15. H. Al Ghoul *et al.*, *AIP Conf. Proc.* **1735**, p. 020001 (2016).
16. D. Mack, *in these proceedings*.
17. C. Gleason, *in these proceedings*.
18. S. Wallner, *in these proceedings*.
19. F. Kaspar, *in these proceedings*.
20. M. Mikhasenko *et al.*, *Eur. Phys. J. C* **78**, 229 (2018).